

Fourier-transform quantum phase estimation with quantum phase noise

François CHAPEAU-BLONDEAU, Étienne BELIN

*Laboratoire Angevin de Recherche en Ingénierie des Systèmes (LARIS),
Université d'Angers, 62 avenue Notre Dame du Lac, 49000 Angers, France.*

Abstract

For the fundamental task of estimating a phase on an arbitrary quantum process, a variant of Fourier-based quantum phase estimation is devised, which uses a probing signal of multiple entangled qubits. For simple practical implementation, each probing qubit can be applied and measured separately. When the qubits are optimally entangled, the Heisenberg enhanced scaling of the estimation efficiency is obtained. The phase estimation protocol can be applied equally in the presence of quantum phase noise. This enables us to investigate the impact of a generic quantum phase noise on the performance of the Fourier-based phase estimation. Especially it reveals that the strategy found optimal with no noise, gradually loses its optimality as the noise increases. Also, in contrast to the noise-free situation, with noise the presence of entanglement is no longer uniformly beneficial to estimation; there exists an optimal amount of entanglement to maximize the efficiency and above which it becomes detrimental. The results contribute to better knowledge of quantum noise and entanglement for quantum signal and information processing.

Key words: Quantum Fourier transform, Quantum estimation, Quantum noise, Quantum signal, Quantum information, Decoherence

1 Introduction

The phase of quantum states can carry useful metrological information [1]. The phase for quantum states is also an essential property which determines their ability for interference, interaction, coherence, and therefrom their capabilities for quantum information processing and computation [1]. Phase estimation on quantum states is therefore a crucial task of quantum metrology, and it relates to other quantum processes where signal processing can usefully contribute [2–8]. For instance, phase estimation at the quantum level is relevant to interferometry, magnetometry, atomic clocks or frequency standards [9,10].

¹ f.chapeau@univ-angers.fr

Phase estimation also stands as a key step in the celebrated Shor quantum algorithm for the prime factorization of integers in polynomial complexity, while all known classical algorithms remain with exponential complexity [11,1,12]. Quantum measurement inherently holds a probabilistic character, and, in the framework of statistical estimation theory, for quantum phase estimation from measurement, various approaches have progressively been developed [13–18].

The Fourier transform is a fundamental tool of signal processing which is intrinsically suited for phase processing. The Fourier transform, when extended to the quantum domain, has been shown to offer the ground for a very efficient and convenient approach to quantum phase estimation [19,20,1]. Reference [19] by Kitaev is commonly recognized as the origin of the Fourier-based approach to quantum phase estimation, while Refs. [20,1] contain further description and analysis of the Kitaev approach. Such Fourier-based approach can deliver a phase estimate with an arbitrary controllable precision, and moreover, as we shall see, by exploiting the specifically quantum property of entanglement, it can achieve enhanced precision inaccessible by classical means [21–24].

Following its proposal, the Fourier-based approach to quantum phase estimation has been analyzed in its principle, and under various feasible forms and variants, especially in the presence of entanglement revealing the possibility of enhanced efficiency [19,20,25,26,23]. For further progress and broader understanding, it is also of primary importance to investigate the behavior of the approach and evolution of its properties, in the realistic conditions where quantum noise is present. Quantum noise – manifesting the decoherence or alteration of quantum states due to their interaction with an uncontrolled environment – is a ubiquitous feature generally impacting the performance of quantum processing and quantum technologies. Very few studies have addressed the analysis of Fourier-based quantum phase estimation in the presence of noise [21,23,27]; and to our knowledge, no studies have been reported on the impact of phase noise, which is specifically meaningful when phase information is at stake, as in the estimation task we consider here.

In this paper we will propose and analyze a variant of the Fourier-based method for quantum phase estimation, and investigate the evolution of its performance in the presence of quantum phase noise. We will start, in Section 2, with a brief recall of the properties required from the quantum Fourier transform. We will then describe in Section 3 the variant of Fourier-based quantum phase estimation, of simple practical implementation and optimizable so as to benefit from enhanced efficiency from quantum entanglement. In addition, in Section 4, this variant will be considered in the presence of quantum phase noise. This will enable us to develop the first analysis of Fourier-based quantum phase estimation in the presence of phase noise, especially offering a handle for investigating the impact of noise on the performance.

2 Quantum Fourier transform

We briefly recall in this Section notions concerning the quantum Fourier transform [1], and that will serve for the methodology of phase estimation. For a quantum system with an N -dimensional complex Hilbert space \mathcal{H}_N , an orthonormal basis is formed by the set of N vectors $|j\rangle \in \{|0\rangle, |1\rangle, \dots, |N-1\rangle\}$ having the Fourier transform

$$|j\rangle \longmapsto |\tilde{j}\rangle = \frac{1}{\sqrt{N}} \sum_{k=0}^{N-1} \exp\left(i2\pi\frac{jk}{N}\right) |k\rangle . \quad (1)$$

The set of the N vectors $\{|\tilde{j}\rangle\} = \{|\tilde{0}\rangle, |\tilde{1}\rangle, \dots, |\widetilde{N-1}\rangle\}$ resulting from Eq. (1) when the integer $j = 0$ to $N - 1$, forms another orthonormal basis of \mathcal{H}_N , and it defines the Fourier transform of the original basis $\{|j\rangle\} = \{|0\rangle, |1\rangle, \dots, |N-1\rangle\}$. The two bases are related through $|\tilde{j}\rangle = U_F |j\rangle$ via the $N \times N$ symmetric unitary matrix U_F with generic term $[\exp(i2\pi jk/N)]/\sqrt{N}$.

The inverse Fourier transform is defined by the reverse change of basis inverting the transformation of Eq. (1) and transforming the Fourier basis $\{|\tilde{j}\rangle\} = \{|\tilde{0}\rangle, |\tilde{1}\rangle, \dots, |\widetilde{N-1}\rangle\}$ back into the original basis $\{|j\rangle\} = \{|0\rangle, |1\rangle, \dots, |N-1\rangle\}$, and reading

$$|\tilde{j}\rangle \longmapsto |j\rangle = \frac{1}{\sqrt{N}} \sum_{k=0}^{N-1} \exp\left(-i2\pi\frac{jk}{N}\right) |\tilde{k}\rangle , \quad (2)$$

or equivalently $|j\rangle = U_F^\dagger |\tilde{j}\rangle$ since by unitarity $U_F^{-1} = U_F^\dagger$.

3 Fourier-based phase estimation

We address the generic problem of quantum phase estimation defined as follows. A quantum process is represented by the unitary operator U_ξ acting in a Hilbert space \mathcal{H} of arbitrary dimension. Being unitary, U_ξ has its eigenvalues of unit modulus in \mathbb{C} ; and U_ξ is endowed with an eigenvalue denoted $\exp(i2\pi\xi)$ associated with the eigenstate $|u\rangle \in \mathcal{H}$, so that $U_\xi |u\rangle = \exp(i2\pi\xi) |u\rangle$. A materialization of the process U_ξ is offered for example by an optical interferometer introducing a phase shift ξ along a path, and operated at the quantum limit, with applications for instance to gravitational wave detection, atomic clocks, or high-sensitivity magnetometry [9,10]. The task is then to estimate the unknown value of the phase $\xi \in [0, 1[$.

As is standard with quantum circuits for quantum processing and computation (see for instance [1] and its Section 4.3), we assume that we can use a qubit in state $|c\rangle$ of the two-dimensional Hilbert space \mathcal{H}_2 , in order to control the application of the unitary U_ξ . This realizes the controlled- U_ξ operation, denoted cU_ξ , and acting in the product space $\mathcal{H}_2 \otimes \mathcal{H}$ as $cU_\xi |c=0\rangle |v\rangle = |c=0\rangle |v\rangle$ and $cU_\xi |c=1\rangle |v\rangle = |c=1\rangle U_\xi |v\rangle$, i.e. the arbitrary state $|v\rangle \in \mathcal{H}$ gets transformed by U_ξ when the control bit $c = 1$, while state $|v\rangle$ remains

unchanged when the control bit $c = 0$. The eigenstate $|u\rangle \in \mathcal{H}$ therefore transforms as $cU_\xi|0\rangle|u\rangle = |0\rangle|u\rangle$ and $cU_\xi|1\rangle|u\rangle = \exp(i2\pi\xi)|1\rangle|u\rangle$.

Based on these elements, several approaches have been proposed for the estimation of the unknown quantum phase ξ . The approach using Fourier transform is specifically useful since it usually involves a single measurement on a multiple-qubit signal to deliver a “one-shot” phase estimate of controllable precision, over the whole feasible range $[0, 1]$ with no need for prior information. The origin of Fourier-based quantum phase estimation is commonly referred to the work of Kitaev [19]; the approach is further analyzed for instance in [20,1] and is briefly reviewed here in Appendix A. This approach by Kitaev [19,20,1], as explained in Appendix A, uses L separable control qubits and $N = 2^L$ evaluations of the elementary process U_ξ in order to estimate the phase ξ with a mean-squared error scaling as $1/N$. This approach by Kitaev in its standard circuit implementation [20,1] uses L distinct gates $U_\xi^{2^\ell}$ obtained by raising U_ξ to all powers of the form 2^ℓ with integer $\ell \in [0, L - 1]$, and moreover under the form of a controlled version of each process $U_\xi^{2^\ell}$. As an alternative here we develop an approach that uses N control qubits and a same number N of evaluations of the elementary process U_ξ , and is able to estimate the phase ξ with the same $1/N$ scaling of the mean-squared error. This approach in its circuit implementation uses only one copy of the elementary controlled- U_ξ process, materialized by a single physical gate for U_ξ , evaluated N times sequentially. In addition, by optimally entangling the N control qubits, an improved mean-squared error scaling as $1/N^2$ instead of $1/N$ will become accessible, as it was also obtained with the Fourier-based estimation of [25,21] in different conditions, but was not present with the original Kitaev approach.

For efficient estimation, we therefore take $N - 1$ control qubits, for which we consider the joint state, denoted $|\bar{k}\rangle$, for integer $k = 0$ to $N - 1$, formed with the k first qubits placed in state $|1\rangle$ while the remaining qubits are placed in state $|0\rangle$, according to

$$|\bar{k}\rangle = \overbrace{|0\rangle \cdots |0\rangle}^N \underbrace{|1\rangle \cdots |1\rangle}_{k}^{N-1} = |\underbrace{0 \cdots 0}_{N-1} \underbrace{1 \cdots 1}_k\rangle. \quad (3)$$

The inner scalar products verifying $\langle \bar{k} | \bar{k}' \rangle = \delta_{kk'}$ for $k, k' = 0$ to $N - 1$, establish that the set of N states $\{|\bar{k}\rangle\}$, for $k = 0$ to $N - 1$, forms an orthonormal basis for the N -dimensional subspace \mathcal{H}'_N of the 2^{N-1} -dimensional Hilbert space $\mathcal{H}_2^{\otimes(N-1)}$ of the $N - 1$ qubits. All the relevant processes that are going to take place will maintain the quantum states in the subspace \mathcal{H}'_N , which is established in this way as the working Hilbert space.

The $N - 1$ qubits in state $|\bar{k}\rangle \in \mathcal{H}'_N$ act as control qubits to the controlled- U_ξ process, as depicted in Fig. 1. Each of the $N - 1$ control qubits is separately physically materialized, and it can therefore be applied sequentially and separately to the controlled- U_ξ gate. In this way, in Fig. 1, the $N - 1$ control qubits are applied sequentially, one after the other, to the same controlled- U_ξ gate fed with the eigenstate $|u\rangle$.

Based on the functioning of the controlled- U_ξ gate described above in this Section, in Fig. 1, in a single step when one control qubit at $|0\rangle$ is applied on the input, one realizes the input–output transformation $|0\rangle|u\rangle \mapsto |0\rangle|u\rangle$, and when one control qubit

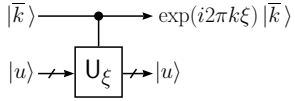


Fig. 1. Quantum circuit involving $N - 1$ input qubits prepared in the state $|\bar{k}\rangle$ of Eq. (3) and acting as control qubits applied sequentially to the controlled- U_ξ gate. The U_ξ gate is fed with its eigenstate $|u\rangle$ which remains unchanged all through the operation. The $N - 1$ control qubits terminate in the joint state $\exp(i2\pi k\xi) |\bar{k}\rangle$ separable from $|u\rangle$, as in Eq. (4).

at $|1\rangle$ is applied, one realizes the input–output transformation $|1\rangle|u\rangle \mapsto \exp(i2\pi\xi)|1\rangle|u\rangle$. Accordingly, when a sequence of $N - 1$ control qubits in state $|\bar{k}\rangle$ are successively applied, one realizes the input–output transformation $|\bar{k}\rangle|u\rangle^{\otimes(N-1)} \mapsto \exp(i2\pi k\xi)|\bar{k}\rangle|u\rangle^{\otimes(N-1)}$. This represents $N - 1$ evaluations of the controlled- U_ξ process, which can be performed sequentially on the same single materialization of the controlled- U_ξ gate, each evaluation triggered in succession by each of the control qubit applied one after the other. This operation realizes a separable evolution of the control qubits and of the arbitrary eigenstate $|u\rangle$, which is similar to the separable evolution occurring in the standard quantum phase estimation approach by Kitaev, as described in Appendix A. As a result, the circuit of Fig. 1 implements, for the $N - 1$ control qubits $|\bar{k}\rangle$, the input–output transformation

$$|\bar{k}\rangle \longmapsto \exp(i2\pi k\xi) |\bar{k}\rangle. \quad (4)$$

Alternatively, instead of the sequential operation described above, an equivalent operation could be carried out in parallel, by applying the $N - 1$ control qubits simultaneously to $N - 1$ controlled- U_ξ gates, at the cost of disposing of $N - 1$ identical controlled- U_ξ gates instead of one in Fig. 1.

The $N - 1$ input control qubits can be prepared in an arbitrary superposition of the

N basis states $\{|\bar{k}\rangle\}$ under the form

$$|\psi_{\text{in}}\rangle = \sum_{k=0}^{N-1} a_k |\bar{k}\rangle , \quad (5)$$

with the complex coefficients $a_k \in \mathbb{C}$ normalized by $\sum_{k=0}^{N-1} |a_k|^2 = 1$. This input probe signal $|\psi_{\text{in}}\rangle \in \mathcal{H}'_N$, by linearity applying on Eq. (4), experiences the input–output transformation

$$|\psi_{\text{in}}\rangle \mapsto \sum_{k=0}^{N-1} a_k \exp\left(i2\pi \frac{j_\xi k}{N}\right) |\bar{k}\rangle = |\tilde{\psi}_\xi\rangle , \quad (6)$$

with $j_\xi = N\xi$.

The probing state $|\tilde{\psi}_\xi\rangle$ of Eq. (6) is clearly dependent on the unknown phase ξ via j_ξ , yet through relative phases between the N complex coordinates of $|\tilde{\psi}_\xi\rangle$. As a result, if $|\tilde{\psi}_\xi\rangle \in \mathcal{H}'_N$ were directly measured in the computational basis $\{|\bar{k}\rangle\}$ of \mathcal{H}'_N , then one would obtain (project on) each possible outcome $|\bar{k}\rangle$ with probability $|a_k|^2$ and nothing could be learned about the phase ξ . Some prior processing has to intervene before measurement. To process the probing state $|\tilde{\psi}_\xi\rangle \in \mathcal{H}'_N$ of Eq. (6) for estimating the phase ξ , an inverse Fourier transform referred to the orthonormal basis $\{|\bar{k}\rangle\}$ of \mathcal{H}'_N is performed on $|\tilde{\psi}_\xi\rangle$. It rests on the inverse Fourier transform of each basis state $|\bar{k}\rangle$ which, according to Eq. (2), reads

$$U_F^\dagger |\bar{k}\rangle = \frac{1}{\sqrt{N}} \sum_{j=0}^{N-1} \exp\left(-i2\pi \frac{jk}{N}\right) |\bar{j}\rangle , \quad (7)$$

to yield

$$U_F^\dagger |\tilde{\psi}_\xi\rangle = |\psi_\xi\rangle = \sum_{j=0}^{N-1} a'_j |\bar{j}\rangle , \quad (8)$$

with the coefficients

$$a'_j = \frac{1}{\sqrt{N}} \sum_{k=0}^{N-1} a_k \exp\left(i2\pi \frac{(j_\xi - j)k}{N}\right) , \quad (9)$$

for $j = 0$ to $N - 1$. The state $|\psi_\xi\rangle \in \mathcal{H}'_N$ of Eq. (8) is then measured in the orthonormal basis $\{|\bar{k}\rangle\}$ of \mathcal{H}'_N .

In the special case of a uniform superposition with all $a_k = 1/\sqrt{N}$ in Eq. (5), and an unknown phase $\xi \in [0, 1[$ yielding $j_\xi = N\xi = j_0$ precisely an integer $j_0 \in [0, N[$, one would have $a'_j = \delta_{jj_0}$ and $|\psi_\xi\rangle = |\bar{j}_0\rangle$ in Eq. (8). The measurement of $|\psi_\xi\rangle$ would then deliver j_0 exactly and therefrom the exact phase $\xi = j_0/N$.

In the generic case of a phase ξ with $j_\xi = N\xi$ non integer, the approach allows us to know ξ with a good precision at $1/N$ resolution. The measurement of $|\psi_\xi\rangle$ in Eq. (8) generally projects on the basis state $|\bar{j}\rangle$ and delivers the integer j with probability $P_j = |a'_j|^2$, for $j = 0$ to $N - 1$. It can be noted that since the basis states $|\bar{k}\rangle$ of Eq. (3) are separable states, the measurement of state $|\psi_\xi\rangle$ with $N - 1$ qubits can in practice be carried out by measuring each of the $N - 1$ qubits separately in the basis $\{|0\rangle, |1\rangle\}$, and then counting the number j of qubits measured (projected) in $|1\rangle$.

The value of the phase is then deduced by² the estimator $\hat{\xi} = j/N$. This leads to the mean-squared estimation error

$$e^2(\hat{\xi}) = \left\langle (\hat{\xi} - \xi)^2 \right\rangle = \sum_{j=0}^{N-1} \left(\frac{j}{N} - \xi \right)^2 P_j . \quad (10)$$

As an alternative, it is also common to compute the estimation error

$$e_s^2(\hat{\xi}) = \frac{1}{\pi^2} \left\langle \sin^2[\pi(\hat{\xi} - \xi)] \right\rangle = \frac{1}{2\pi^2} \left[1 - \left\langle \cos[2\pi(\hat{\xi} - \xi)] \right\rangle \right] , \quad (11)$$

also considered for instance in [28,25,21,23]. The error of Eq. (11) is more tractable analytically; also it is well suited for an angle parameter encompassing some periodicity: a change of 2π or its multiple in the true phase angle does not physically affect the operation of the quantum process U_ξ under estimation, and accordingly Eq. (11) is not affected in such circumstance. And most importantly, Eq. (11) coincides with the standard mean-squared error of Eq. (10) in the meaningful range of small error that is primarily of interest for the estimation task here.

For a useful reference, again we can first particularize to the case of a uniform superposition $a_k = 1/\sqrt{N}$ in Eq. (5). The sum of Eq. (9) can then be explicitly carried out to give

$$a'_j = \exp \left[i\pi \frac{N-1}{N} (j_\xi - j) \right] \frac{1}{N} \frac{\sin[\pi(j_\xi - j)]}{\sin[\pi(j_\xi - j)/N]} . \quad (12)$$

The measurement probability $P_j = |a'_j|^2$ then readily follows, and the estimation error of Eq. (11) evaluates to

$$e_s^2(\tilde{\xi}) = \frac{1}{2\pi^2 N} [1 - \cos(2\pi j_\xi)] = \frac{1}{\pi^2 N} \sin^2(\pi j_\xi) , \quad (13)$$

with also $e^2(\tilde{\xi}) \approx e_s^2(\tilde{\xi})$ at large N when the error is small. From Eq. (13) we recover the vanishing estimation error expected when $j_\xi = j_0$ precisely an integer. Otherwise, in the generic case, Eq. (13) leads to a mean-squared estimation error evolving as $e^2(\tilde{\xi}) \sim 1/N$, known as the shot-noise or standard scaling of the error. This performance of a mean-squared estimation error decreasing as $1/N$ is similar to what can be expected classically with a number $\sim N$ of measured qubits involved in $\sim N$ evaluations of the process U_ξ to be estimated. With the same number $\sim N$ of evaluations of the process U_ξ , it is the same $1/N$ shot-noise scaling of the mean-squared estimation error which is obtained with the original approach by Kitaev [19,20,1] that uses separable qubits, as explained in Appendix A. By contrast, the $N-1$ qubits in the input signal $|\psi_{in}\rangle$ of Eq. (5) are generally entangled. By adjusting the coefficients a_k of the input superposition in Eq. (5), we are going to show that it is possible to optimally entangle the $N-1$ qubits of $|\psi_{in}\rangle$ so as to obtain a striking improvement of the estimation error. This optimization will

² For a given j the probability $P_j = |a'_j|^2$ resulting from Eq. (9) seen as a function of ξ represents the likelihood, and maximized by $\xi = j/N$ it establishes $\hat{\xi} = j/N$ as the maximum likelihood estimator.

allow us to reach the so-called Heisenberg scaling of the error, with a mean-squared error decreasing as $1/N^2$ instead of $1/N$. For Fourier-based quantum phase estimation, as we address here, such Heisenberg scaling of the error has previously been obtained in [25,21], in two distinct sets of conditions also differing from those considered here.

Instead of a uniform superposition $a_k = 1/\sqrt{N}$ in Eq. (5), we seek to optimize the coefficients a_k in Eq. (5), in order to minimize the estimation error resulting from measuring $|\psi_\xi\rangle$ of Eq. (8). This is undertaken in Appendix B, where the estimation error $e_s^2(\hat{\xi})$ from Eq. (11) is explicitly evaluated with arbitrary coefficients $a_k \in \mathbb{C}$ in Eq. (5). It is then found in Eq. (B-13) that minimization of the error $e_s^2(\hat{\xi})$ is accomplished by the optimal coefficients

$$a_k = \sqrt{\frac{2}{N}} \sin\left(\pi \frac{k}{N}\right), \quad k = 0, 1, \dots, N-1, \quad (14)$$

achieving in Eq. (11) via Eq. (B-17) the minimal error

$$e_s^2(\hat{\xi}) = \frac{1}{\pi^2} \sin^2\left(\frac{\pi}{2N}\right). \quad (15)$$

Especially, at large size N , the estimation error $e_s^2(\hat{\xi})$ of Eq. (15) coincides with the mean-squared error $e^2(\hat{\xi})$ of Eq. (10) which comes out as $e^2(\hat{\xi}) \approx 1/(4N^2)$.

We observe here the striking benefit that can be obtained from an optimally entangled superposition in $|\psi_{\text{in}}\rangle$ of Eq. (5) for probing the quantum process U_ξ under estimation. With $\sim N$ evaluations of the process U_ξ , the uniform superposition in $|\psi_{\text{in}}\rangle$ achieves, as we have seen based on Eq. (13), a mean-squared error evolving as $1/N$, and this is a standard scaling also achieved in classical parameter estimation from N independent measurements. By contrast, for $|\psi_{\text{in}}\rangle$ the nonuniform optimal superposition from Eq. (14) is able to achieve a much reduced mean-squared estimation error evolving as $1/N^2$. This so-called Heisenberg scaling of the error constitutes a specifically quantum improvement, with no classical equivalent.

The proposed Fourier-based estimation scheme with the $1/N^2$ efficiency here bears similarity with the schemes analyzed in [25,21]. All three schemes share the same $1/N^2$ Heisenberg scaling of the mean-squared estimation error, obtained by a comparable optimization of a multiple-qubit excitation signal. References [25,21] however deal with phase estimation on a single qubit gate, with a probing signal of N qubits that are directly processed by the one-qubit gate to be estimated. By contrast, our approach deals with phase estimation on an arbitrary quantum process U_ξ (not necessarily a qubit process), which interacts with a signal of $N-1$ auxiliary qubits acting as control to U_ξ for the phase estimation. In the end, the optimal configuration of the amplitudes a_k of the multiple-qubit signal turns out to be similar, but its applicability and significance get broaden in this respect. Another difference is that the criterion optimized in [25] is an estimation error averaged over all values of the phase ξ to be estimated according to a uniform prior. Meanwhile, in [21] and in our study it is established that the optimal a_k 's (the same as in [25]) minimize the error for every value of the phase ξ , and these accordingly will minimize the error averaged over any prior (not necessarily uniform). Another slight difference is

that the optimization here is performed over the broader condition of complex coefficients $a_k \in \mathbb{C}$, while optimization is over real a_k 's in [21]; but in the end we show here that the optimal a_k 's turn out to be real, so the difference has no impact on the solution, except that we know that complex a_k 's do not help. Another specificity here is that the $(N - 1)$ -qubit excitation signal $|\psi_{\text{in}}\rangle$ of Eq. (5) is constructed as a superposition of basis states $|\bar{k}\rangle$ that are somewhat simpler than in [21]. This will become especially relevant in the sequel, when we will introduce a scenario to analyze the impact of quantum noise on the performance of the Fourier-based estimation.

4 Fourier-based estimation with noise

We now consider that the $N - 1$ control qubits, before they become accessible for their processing to estimate the phase ξ , are affected by quantum noise according to the diagram of Fig. 2.

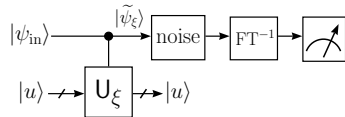


Fig. 2. The input signal $|\psi_{\text{in}}\rangle$ from Eq. (5) with $N - 1$ qubits, after acting as control to the U_ξ gate as in Fig. 1, is transformed into the state $|\tilde{\psi}_\xi\rangle$ of Eq. (6). Then this probing state $|\tilde{\psi}_\xi\rangle$ is affected by quantum noise before being processed by inverse Fourier transform and measurement to estimate the phase ξ .

4.1 Analytical modeling

We analyze here, on the $N - 1$ control qubits of probe signal, the effect of a phase-flip noise also known as phase damping noise. Such phase-flip noise is an important quantum noise that acts on the qubit [1,4]. It can represent many decohering processes that can affect the qubit: for instance how a photon is randomly scattered as it propagates, or how an electron may be perturbed by interacting with distant electric charges [1]. Such phase noise is specially meaningful in this context where we are targeting to recover (estimate) a phase information. We will also show that its effect on the Fourier-based phase estimation can be theoretically analyzed rather thoroughly. This is specially useful because very few analyses have previously been reported on the effect of quantum noise on Fourier-based phase estimation.

The phase-flip noise acting on a qubit in the generic state $|\phi\rangle = \alpha_0|0\rangle + \alpha_1|1\rangle \in \mathcal{H}_2$ has the effect of randomly flipping the relative phase of its two complex coordinates in \mathcal{H}_2 so as to produce the state $\alpha_0|0\rangle - \alpha_1|1\rangle$ with probability p , while the state remains unchanged with probability $1 - p$. Such a phase flip can be modeled with the unitary Pauli operator $\sigma_z = |0\rangle\langle 0| - |1\rangle\langle 1|$ acting in \mathcal{H}_2 . So with probability p the state $|\phi\rangle$ is replaced by the state $\sigma_z|\phi\rangle$. An initial pure state $|\phi\rangle$, by the action of the phase-flip noise, becomes a mixed state, equivalent to the two-state statistical ensemble $\{(|\phi\rangle, 1 - p), (\sigma_z|\phi\rangle, p)\}$ comprising state $|\phi\rangle$ with probability $1 - p$ and state $\sigma_z|\phi\rangle$ with probability p . A noisy qubit in such a mixed state can be handled by means of the density operator $\rho = (1 - p)|\phi\rangle\langle\phi| + p\sigma_z|\phi\rangle\langle\phi|\sigma_z^\dagger$, yet, as an equivalent alternative, we find it more convenient here to explicitly work out the conditional statistics resulting from the two-state statistical ensemble.

We focus on the basis state $|\bar{k}\rangle \in \mathcal{H}'_N$ of Eq. (3) occurring in the probing state $|\tilde{\psi}_\xi\rangle$ of Eq. (6), when a phase-flip noise can affect independently each of the $N - 1$ qubits of $|\bar{k}\rangle$. By the action of the phase-flip noise, in each basis state $|\bar{k}\rangle$ of Eq. (3) with $N - 1$ qubits, a state $|0\rangle$ remains unchanged while a state $|1\rangle$ is changed to $-|1\rangle$ with probability p . In this way, by the action of the noise, each $|\bar{k}\rangle$ can be changed to $\pm|\bar{k}\rangle$ and stays in the space \mathcal{H}'_N . In the state $|\bar{k}\rangle$, among the k states $|1\rangle$, a number $f \in [0, k]$ of flips occurs with the probability $p_f = C_f^k p^f (1 - p)^{k-f}$ of the binomial law, with the binomial coefficient $C_f^k = k!/[f!(k - f)!]$. The state $|\bar{k}\rangle$ becomes $-|\bar{k}\rangle$ when an odd number of flips occurs among k , and this takes place with probability $F(k)$ obtained by summing p_f over all odd f between 1 et k . We shall also note $1 - F(k) = \bar{F}(k)$ the complementary probability when $|\bar{k}\rangle$ remains $|\bar{k}\rangle$.

The probing state $|\tilde{\psi}_\xi\rangle$ of Eq. (6) with its $N - 1$ qubits is now affected by the phase-flip noise, as depicted in Fig. 2. To work out the effect of the noise on $|\tilde{\psi}_\xi\rangle$, it is convenient in Eq. (6) to write $|\tilde{\psi}_\xi\rangle = \sum_{k=0}^{N-1} b_k |\bar{k}\rangle$ with $b_k = a_k \exp(i2\pi j_\xi k/N)$. In the transformation $|\bar{k}\rangle \mapsto \pm|\bar{k}\rangle$ by the noise, only the state $|\bar{0}\rangle$ is unaffected, while every other basis state $|\bar{k}\rangle$ experiences a change of its sign with probability $F(k)$. In this way, according to the pattern of changes of sign enforced by the noise over the $N - 1$ basis states $|\bar{k}\rangle$, the probing state $|\tilde{\psi}_\xi\rangle$ gets transformed into a statistical ensemble of 2^{N-1} states of the form $\sum_{k=0}^{N-1} b'_k(\ell) |\bar{k}\rangle = |\psi'_\ell\rangle \in \mathcal{H}'_N$ endowed with probabilities P'_ℓ , where $b'_k(\ell) = \pm b_k$ for $\ell = 1$

to 2^{N-1} . Each value of ℓ identifies one pattern of (change of) signs which is feasible on the $N - 1$ basis states $|\bar{k}\rangle$ occurring in $|\tilde{\psi}_\xi\rangle$.

For instance, from $|\tilde{\psi}_\xi\rangle = b_0 |\bar{0}\rangle + b_1 |\bar{1}\rangle + \cdots + b_{N-1} |\bar{N-1}\rangle$, the configuration $\ell = 1$ would be the configuration with no change of sign, when $|\tilde{\psi}_\xi\rangle$ remains $|\tilde{\psi}_\xi\rangle = |\psi'_1\rangle$ and $b'_k(\ell = 1) = b_k$ for all $k = 0$ to $N - 1$, this configuration occurring with the probability $P'_{\ell=1} = \bar{F}(1)\bar{F}(2)\cdots\bar{F}(N-1)$. The configuration $\ell = 2$ would be the configuration with one change of sign, when $|\tilde{\psi}_\xi\rangle$ becomes $|\psi'_2\rangle = b_0 |\bar{0}\rangle - b_1 |\bar{1}\rangle + \cdots + b_{N-1} |\bar{N-1}\rangle$, and $b'_1(\ell = 2) = -b_1$ while for all other $b'_k(\ell = 2) = b_k$, this configuration occurring with the probability $P'_{\ell=2} = F(1)\bar{F}(2)\cdots\bar{F}(N-1)$. There is a total of $N - 1$ such configurations implementing on $|\tilde{\psi}_\xi\rangle$ one change of sign. In a similar way, the configurations implementing on $|\tilde{\psi}_\xi\rangle$ from 2 up to $N - 1$ changes of sign are readily enumerated with their corresponding probabilities P'_ℓ . For example, the configuration with two changes of sign transforming $|\tilde{\psi}_\xi\rangle$ into $|\psi'_\ell\rangle = b_0 |\bar{0}\rangle - b_1 |\bar{1}\rangle + \cdots - b_{N-1} |\bar{N-1}\rangle$ would occur with the probability $P'_\ell = F(1)\bar{F}(2)\cdots\bar{F}(N-2)F(N-1)$. This leads to a complete characterization of the statistical ensemble $\{(|\psi'_\ell\rangle, P'_\ell)\}$ representing the probing state $|\tilde{\psi}_\xi\rangle$ of Eq. (6) after it has been affected by the phase-flip noise as in Fig. 2. This statistical ensemble $\{(|\psi'_\ell\rangle, P'_\ell)\}$ is easily listed and processed numerically, as we will do in Section 4.2. By contrast, the associated density operator would be rather explosive and cumbersome to handle analytically.

We also emphasize that, since the phase noise acts on the basis states $|\bar{k}\rangle$ of the N -dimensional space \mathcal{H}'_N according to $|\bar{k}\rangle \mapsto \pm |\bar{k}\rangle \in \mathcal{H}'_N$, then the probing state $|\tilde{\psi}_\xi\rangle$ of Eq. (6) after it has been affected by the noise as in Fig. 2, remains in the same space \mathcal{H}'_N . The same processing in \mathcal{H}'_N , as in the noise-free situation of Section 3, can therefore be applied in presence of the phase noise, as depicted in Fig. 2. This is an important property, obtained here by specifically preparing the $N - 1$ control qubits in the input state $|\psi_{\text{in}}\rangle \in \mathcal{H}'_N$ of Eq. (5) as the input probe. Other probes may not have this invariance property, as for instance the $(N - 1)$ -qubit probe used in [21], which starts in an N -dimensional subspace as our $|\psi_{\text{in}}\rangle$ of Eq. (5), but which by the action of a phase noise as the one we consider here, would end up in the whole 2^{N-1} -dimensional space of the $N - 1$ qubits. This then precludes to realize the same processing in an N -dimensional noise-free and in a 2^{N-1} -dimensional noisy situations, and calls for a modified estimation protocol to handle the noisy situation. By contrast here, with the probe signal $|\psi_{\text{in}}\rangle$ of Eq. (5), the same estimation protocol applies without and with noise, and as such it lends itself to a noise analysis.

Here, on the $N - 1$ noisy qubits ending up in a mixed quantum state represented by the statistical ensemble $\{(|\psi'_\ell\rangle, P'_\ell)\}$, the same N -dimensional inverse Fourier transform as in Eq. (8) is applied, as depicted in Fig. 2. In the inverse Fourier transform, each state $|\psi'_\ell\rangle = \sum_{k=0}^{N-1} b'_k(\ell) |\bar{k}\rangle \in \mathcal{H}'_N$ of the statistical ensemble $\{(|\psi'_\ell\rangle, P'_\ell)\}$ becomes

$$U_F^\dagger |\psi'_\ell\rangle = \sum_{j=0}^{N-1} c_j(\ell) |\bar{j}\rangle \in \mathcal{H}'_N , \quad (16)$$

with the coefficients

$$c_j(\ell) = \frac{1}{\sqrt{N}} \sum_{k=0}^{N-1} b'_k(\ell) \exp\left(-i2\pi \frac{jk}{N}\right) = \text{FT}\left[b'_k(\ell)\right], \quad (17)$$

also maintaining the state in the space \mathcal{H}'_N .

Then, as before in the noise-free situation of Section 3, the $N - 1$ qubits are subjected to a projective measurement in the orthonormal basis $\{|\bar{k}\rangle\}$ of \mathcal{H}'_N , as depicted in Fig. 2. The squared modulus $|c_j(\ell)|^2$ alone is the (conditional) probability of projecting on state $|\bar{j}\rangle$ conditioned on the noisy probe being in the state $|\psi'_\ell\rangle$ of the statistical ensemble, this occurring with the probability P'_ℓ previously worked out. The total probability of a measurement projecting on state $|\bar{j}\rangle$ is then

$$P_j = \sum_{\ell=1}^{2^{N-1}} |c_j(\ell)|^2 P'_\ell. \quad (18)$$

Finally, the same estimator $\hat{\xi} = j/N$ is used as in the noise-free situation of Section 3, which follows with a similar mean-squared error $e^2(\hat{\xi}) = \langle (\hat{\xi} - \xi)^2 \rangle$ as in Eq. (10).

4.2 Numerical analysis

The discrete sums of Eqs. (17) and (18) are then evaluated numerically while keeping track of the discrete set of configurations of the statistical ensemble $\{(|\psi'_\ell\rangle, P'_\ell)\}$. This final numerical step is in some sense exact and is used to obtain explicit access to the mean-squared error $e^2(\hat{\xi}) = \langle (\hat{\xi} - \xi)^2 \rangle$ resulting from the theoretical analysis of Section 4.1. This allows us to investigate the impact of the phase-flip noise on the performance of the Fourier-based phase estimation. Figure 3 displays the evolution of the root-mean-squared (rms) error $e(\hat{\xi})$ as a function of the flip probability p of the phase-flip noise, for two values of N controlling the size of the multiple-qubit probe. Figure 3 is obtained with the optimal coefficients a_k of Eq. (14) in the $(N - 1)$ -qubit excitation signal $|\psi_{\text{in}}\rangle$ of Eq. (5). In Fig. 3 and later, the performance is evaluated while estimating the phase $\xi = 0.5 + 0.5/N$ so as to test the most severe condition when $N\xi$ can be maximally distant from an integer j_0 , although this choice is not critical for an assessment of the performance.

Consistently in Fig. 3 the estimation error $e(\hat{\xi})$ increases as the noise probability p grows, with first a steep increase of $e(\hat{\xi})$ for small p rising above zero, and a saturation of $e(\hat{\xi})$ as p approaches $1/2$. A larger size N corresponds to a finer resolution in the phase estimation, and accordingly Fig. 3 shows a smaller estimation error for larger N at any noise level p . When p goes to zero in Fig. 3, the rms error meets the value $e(\hat{\xi}) = 1/(2N)$ expected from the noise-free situation of Section 3.

We also test the performance with uniform coefficients $a_k = 1/\sqrt{N}$ in the input superposition $|\psi_{\text{in}}\rangle$ of Eq. (5). Figure 4 compares the performance of such a uniform $|\psi_{\text{in}}\rangle$ with that of the optimal $|\psi_{\text{in}}\rangle$ resulting from Eq. (14).

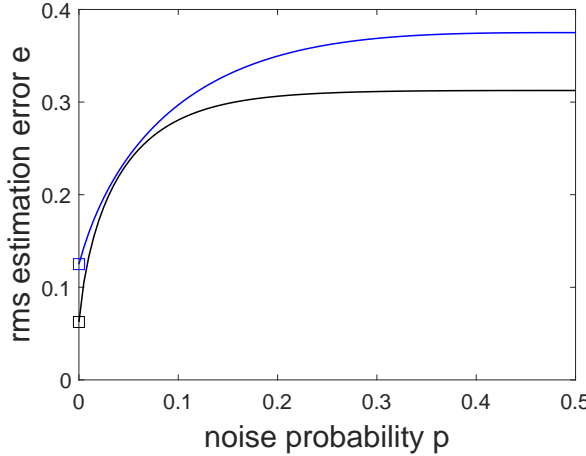


Fig. 3. Rms estimation error $e(\hat{\xi})$ as a function of the flip probability p of the phase-flip noise, for two sizes $N = 4$ (upper curve) and $N = 8$ (lower curve). The input superposition $|\psi_{\text{in}}\rangle$ in Eq. (5) is with the optimal coefficients a_k from Eq. (14). The two squares at $p = 0$ are the rms error $e(\hat{\xi}) = 1/(2N)$ expected at no noise from Section 3.

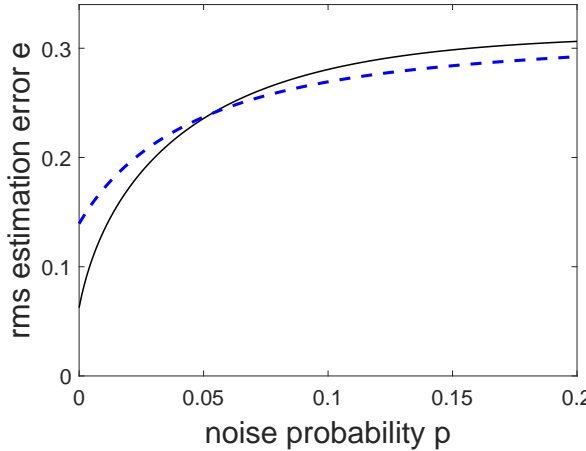


Fig. 4. Rms estimation error $e(\hat{\xi})$ as a function of the flip probability p of the phase-flip noise, at the size $N = 8$, and for an input superposition $|\psi_{\text{in}}\rangle$ in Eq. (5) with the optimal coefficients a_k from Eq. (14) (solid line), or with the uniform coefficients $a_k = 1/\sqrt{N}$ (dashed line).

In Fig. 4, at small noise when $p \rightarrow 0$, as expected the optimal input superposition from Eq. (14) is more efficient with a smaller estimation error compared to the uniform input superposition. However, this superiority gradually diminishes as the noise probability p increases. A crossover is observed around $p \approx 0.05$ in the conditions of Fig. 4, above which the uniform superposition becomes more efficient with a smaller error compared to the optimal superposition (devised to be optimal at zero noise). With the present theory it can further be found that the value of the crossover for p is slightly dependent on the size N characterizing the probe signal $|\psi_{\text{in}}\rangle$: as N increases, the crossover value for p decreases. In this way, as the noise increases, the optimality at zero noise disappears more rapidly for larger probe signals. This is consistent with the character often observed that larger entangled signals are more fragile to noise. In addition in Fig. 4, at the limit $p \rightarrow 1/2$, the two configurations of the input superposition $|\psi_{\text{in}}\rangle$ are equally affected by the noise and tend to saturate at the same estimation error.

The results of Fig. 4 therefore indicate that the input distribution of the coefficients a_k in Eq. (14), optimal at $p = 0$ to achieve the minimal estimation error, then ceases to be optimal as the noise probability p increases. This in principle opens the possibility of seeking to re-optimize at each noise level p the coefficients a_k . But this is a much involved optimization task, especially in the presence of a large cardinality 2^{N-1} of the statistical ensemble $\{(\lvert\psi'_\ell\rangle, P'_\ell)\}$ representing the noisy probing state, and we know of no analytical solution comparable to the one of Eq. (14) with no noise. Pragmatically, the configurations of Fig. 4 with noise offer conditions allowing an effective phase estimation, although not necessarily optimal, and this by indicating, according to the noise level p , when to switch the input coefficients a_k from the distribution of Eq. (14) to the uniform distribution so as to keep the estimation error small.

Another interesting aspect accessible with the present treatment, is to analyze the impact of the size N controlling the size of the $(N - 1)$ -qubit probe prepared in the entangled state $\lvert\psi_{\text{in}}\rangle$ of Eq. (5). For this purpose, Fig. 5 represents the evolution of the rms estimation error $e(\hat{\xi})$ as a function of the size N , and at various values of the flip probability p of the phase-flip noise.

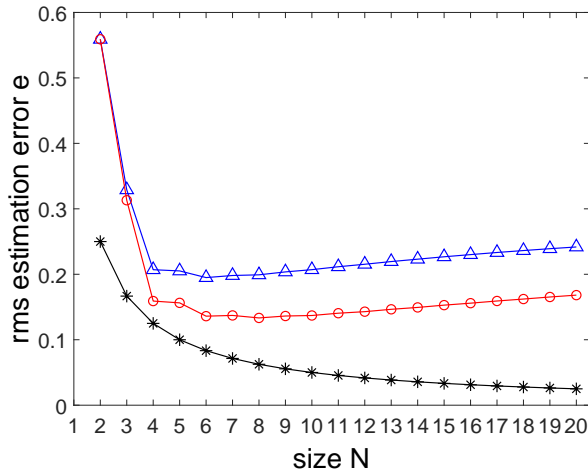


Fig. 5. Rms estimation error $e(\hat{\xi})$ as a function of the size N controlling the size of the $(N - 1)$ -qubit probe prepared in the state $\lvert\psi_{\text{in}}\rangle$ of Eq. (5). The input superposition $\lvert\psi_{\text{in}}\rangle$ in Eq. (5) is with the optimal coefficients a_k from Eq. (14). With (*) for $e(\hat{\xi}) = 1/(2N)$ representing the noise-free situation of Section 3. With the phase-flip noise, of flip probability $p = 0.01$ (○) and $p = 0.03$ (△).

At no noise at $p = 0$ in Fig. 5 is the noise-free situation of Section 3, when the rms estimation error $e(\hat{\xi}) = 1/(2N)$ decreases as $1/N$ with an increasing size N . Notably, as previously indicated, this is a specifically quantum performance, inaccessible with classical means: Classically, statistical estimation with N successive measurements is maximally efficient with N independent measurements to yield an rms error evolving as $\sim 1/\sqrt{N}$. The better quantum performance here, with an rms error evolving as $\sim 1/N$, is made possible through optimized entanglement of the $N - 1$ qubits of the input probe according to Eq. (14).

In the presence of noise however, the results of Fig. 5 show that the benefit of entanglement does not uniformly increase with increasing entanglement size N . On the

contrary, at $p \neq 0$, there is an optimum for the entanglement size N , between 6 and 8 in the conditions of Fig. 5, above which the estimation error no longer decreases but instead slowly increases with increasing N . The existence of such finite optimal entanglement size N_{opt} is observed in Fig. 5 with the optimal input superposition from Eq. (14), however the same property is observed at comparable values with a uniform input superposition. For each condition and noise level, the present analysis allows one to predict the optimal entanglement size N_{opt} for estimation.

In the presence of noise with a finite optimal entanglement size N_{opt} , a useful approach to further improve the efficiency would be to fix the size of the input probe at N_{opt} , and then to repeat several (M) times the estimation experiment to obtain the estimates $\hat{\xi} = \hat{\xi}_m$ that would be finally averaged as $\sum_{m=1}^M \hat{\xi}_m / M$. Increasing M allows the possibility of gradually reducing the estimation error, and most rapidly when operating at the optimal size N_{opt} .

The results of Fig. 5 reveal the versatile role of entanglement as a specific quantum correlation. With no noise, entanglement is always beneficial to the estimation performance and its efficiency uniformly increases as the entanglement size N increases. By contrast, in the presence of noise, entanglement is beneficial up to a certain value of the size N , above which it becomes detrimental with a performance that decreases as N further increases. The quantum correlation across entangled qubits provides a coordinated response which is useful to extract information about the unknown phase or to combat the noise, up to a certain optimal size of entanglement. At larger entanglement size, the correlation drives the qubits too much in the direction of the noise, and the collective response gets dominated by the noise with no benefit for information processing.

5 Discussion

For estimating a phase ξ on an arbitrary quantum process U_ξ , we have devised a variant of Fourier-based quantum phase estimation, especially using a probing signal made of $N - 1$ control qubits entangled in the quantum state $|\psi_{\text{in}}\rangle$ of Eq. (5). A practically appealing feature is that these $N - 1$ qubits can be applied one by one sequentially to probe the process U_ξ under estimation, and they can also be measured one by one separately. We have especially shown that by optimally entangling the input superposition $|\psi_{\text{in}}\rangle$ of Eq. (5) by means of the optimal coefficients a_k of Eq. (14), it is possible to achieve the improved Heisenberg scaling as $1/N^2$ of the mean-squared estimation error, in place of the standard scaling as $1/N$.

The present algorithm for quantum phase estimation is based on the standard notion of quantum Fourier transform (QFT) attached to an orthonormal basis of an Hilbert space with dimension N , as expressed by Eq. (1). Beyond the algorithmic level forming the focus of this study, the practical physical implementation of the QFT is a non trivial issue in its own right, with relevance to many other quantum algorithms and still open for research. An efficient physical implementation is known for the QFT over the full Hilbert space of N qubits with dimension 2^N , i.e. when the dimension is a power of

two [1]. The QFT of our algorithm operates in the N -dimensional subspace \mathcal{H}'_N spanned by the orthonormal basis $\{|\bar{k}\rangle\}$ from Eq. (3). This is a similar situation with the QFT-based approach by [21] that we mentioned earlier. It is assured in principle that such N -dimensional QFT is physically implementable for any N since it represents a valid unitary operation, and moreover it is implementable by a combination of one-qubit gates and two-qubit Cnot gates known to form a universal set of gates for quantum circuits [1]. However, the standard implementation of the 2^N -dimensional QFT over the full Hilbert space may not apply directly. Different possibilities are accessible to address this situation. In the case where $N = 2^K$ is itself a power of two, the standard 2^K -dimensional QFT implementation can be used, provided a change of basis from $\{|\bar{k}\rangle\}$ to the canonical basis of K qubits is first realized, followed by the inverse change of basis after operation of the QFT. An additional possibility could be to consider the approach of [29] investigating a physical implementation of the QFT which differs from the standard QFT circuit on the full 2^N -dimensional Hilbert space of N qubits, and which is not constrained by a power-of-two dimensionality. Also, the physical implementation of a generic quantum algorithm strongly depends on the physical materialization of the quantum states especially the canonical basis states of the representation. It can be noted that, for the postprocessing of the probing state $|\tilde{\psi}_\xi\rangle$ of Eq. (6), with a photonic implementation if the representation changes from quantum states based on polarization qubits to quantum states based on photon number like optical Fock states, then the N photon states $|\bar{k}\rangle$ of Eq. (3) now form the N canonical basis states $\{|0\rangle, |1\rangle, |2\rangle, \dots, |N-1\rangle\}$ of the photon-number representation. Such photonic quantum states come with additional specific possibilities for the QFT implementation, notably with linear optics [30]. Ultimately, it relates to quantum compilers to adapt generic quantum algorithms to specific material processors; hopefully this step will be made transparent by future quantum compilers currently under development [31,32] and decouple the algorithmic and implementation levels.

At the algorithmic level, other techniques are known to achieve the optimal Heisenberg scaling of the estimation precision, by relying on so-called GHZ states for qubits comparable to NOON states of photons [21,22]. Such an N -qubit NOON state here would correspond to an equiweighted entangled superposition of all the N qubits in state $|0\rangle$ and all the N qubits in state $|1\rangle$ as

$$|\psi_{\text{in}}\rangle = \frac{1}{\sqrt{2}} \left(|\underbrace{0 \cdots 0}_N\rangle + |\underbrace{1 \cdots 1}_N\rangle \right), \quad (19)$$

which, after acting on the controlled-U $_\xi$ process, would terminate in the state

$$|\tilde{\psi}_\xi\rangle = \frac{1}{\sqrt{2}} \left(|0 \cdots 0\rangle + \exp(i2\pi N\xi) |1 \cdots 1\rangle \right). \quad (20)$$

This performs what is known as parameter amplification, when the N -qubit probing state $|\tilde{\psi}_\xi\rangle$ of Eq. (20) is now dependent on the amplified parameter $N\xi$. Such NOON states as in Eq. (20) achieve the highest phase resolution possible for a given number N of qubits, with Heisenberg scaling; but they do not provide an unambiguous phase estimate. The reason is that it is the amplified parameter $N\xi$ which is deducible as an estimate over $[0, 1]$ from the probing state $|\tilde{\psi}_\xi\rangle$ of Eq. (20). By dividing by N this estimate, N possible determinations

result for the phase ξ over $[0, 1[$, differing by n/N with integer $n = 0, 1, \dots, N - 1$. This ambiguity can be lifted only with prior or additional information on the phase, or with techniques more involved than measuring only one single response from one N -qubit NOON state excitation – possibly adaptive techniques or repeated measurements from several preselected excitations [21,22,33]. Also, possibly, the ambiguity will not happen in “local” estimation, when one seeks to estimate, with a high quantum precision, a very small change around a priorly known phase [34].

By contrast, an excitation like $|\psi_{\text{in}}\rangle$ of Eq. (5) is able to probe, via the response $|\tilde{\psi}_\xi\rangle$ of Eq. (6), a whole range of phase multiples $k\xi$ with integer $k \in [0, N[$, and which after inverse Fourier transform as we have seen, enables to recover unambiguously one single value for the phase estimate in $[0, 1[$. It is this valuable property of unambiguous global phase estimation which is made possible by the Fourier-based approach.

The above properties were observed in the absence of quantum noise, and as such they stand as useful references for assessing and comparing the capabilities of various approaches to quantum phase estimation. As a complement here, our variant of Fourier-based quantum phase estimation was also analyzed in the presence of quantum phase noise. We investigated the impact on the estimation performance, of a generic phase-flip or phase damping noise acting on the probing qubits. Very few comparable scenarios of Fourier-based quantum phase estimation with noise have ever been reported. Other reports such as [35–38] also addressed quantum phase estimation with noise, but with differing approaches, estimation techniques, performance evaluation or noise models. None of them reached better efficiency beyond the Heisenberg scaling of the estimation error we obtain here, and none addressed Fourier-based quantum phase estimation with quantum phase noise as we do here. All these studies are in fact complementary on the fundamental problem of quantum phase estimation with noise and its various aspects.

Our study, as a significant feature, revealed that the nonuniform input superposition from Eq. (14), proven to be optimal for minimum-error estimation with no noise, ceases to be optimal as the noise level increases above zero. At larger noise level, the uniform input superposition catches up and comes to perform better with a smaller estimation error. A comparable behavior was observed in [24], on another approach to quantum estimation and another performance metric, and where the optimum at no noise also ceases to hold as the noise level increases, although the optimal solution at each noise level remains difficult to characterize. This confirms that quantum noise is an important feature to explicitly include in analyses of quantum information, because efficient strategies without and with noise may differ, even though with noise the characterization gets more complicated, yet good suboptimal alternatives may then be identified.

Another significant feature observed here is that, in contrast to the noise-free situation, with noise the presence of entanglement is no longer uniformly beneficial for information processing. There exists an optimal size for entangled states – which can be determined by the present analysis according to the conditions –, and larger entanglement sizes would become detrimental to the performance. This type of optimum at a finite size of entanglement in the presence of noise, was also observed in [39–41] for other scenarios of quantum metrology or estimation. It manifests the sophisticated role of entanglement

for quantum information processing in the presence of noise, which largely remains to be explored.

The present study combining entanglement and noise for Fourier-based phase estimation in this way represents a useful proposal to contribute to better knowledge and mastering for quantum signal and information processing.

Appendix A: Standard Fourier-based quantum phase estimation

We briefly recall here the standard Fourier-based approach for quantum phase estimation, having its origin in [19], and later examined in [20] or [1] for instance. This approach requires to have access to the process U_ξ when raised to any power of the form 2^ℓ for L values of the integer $\ell \in [0, L - 1]$, i.e. as $U_\xi^{2^\ell}$. This is usually achievable by appropriately cascading multiple copies of the process U_ξ . Application to the eigenstate $|u\rangle \in \mathcal{H}$ yields $U_\xi^{2^\ell} |u\rangle = \exp(i2\pi2^\ell\xi) |u\rangle$. With access also to a controlled version of each process $U_\xi^{2^\ell}$, one is able to perform the state transformation from $\mathcal{H}_2 \otimes \mathcal{H}$ onto $\mathcal{H}_2 \otimes \mathcal{H}$,

$$\frac{1}{\sqrt{2}}(|0\rangle + |1\rangle) |u\rangle \mapsto \frac{1}{\sqrt{2}}[|0\rangle + \exp(i2\pi2^\ell\xi) |1\rangle] |u\rangle . \quad (\text{A-1})$$

In this transformation, an input control qubit of \mathcal{H}_2 is placed in the state $(|0\rangle + |1\rangle)/\sqrt{2} = |+\rangle$, and this qubit terminates in the separable state $[|0\rangle + \exp(i2\pi2^\ell\xi) |1\rangle]/\sqrt{2}$ in the right-hand size of Eq. (A-1). A number L of such control qubits prepared in state $|+\rangle$ are then used according to the setting depicted in Fig. 6.

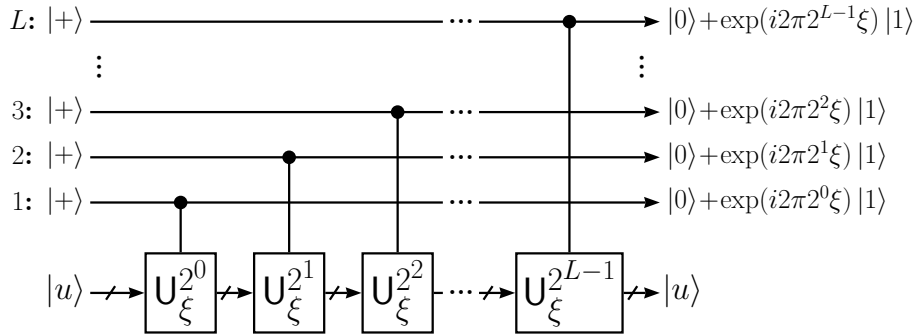


Fig. 6. Quantum circuit involving L input qubits prepared in state $|+\rangle$ and acting as control qubits to the controlled- $U_\xi^{2^\ell}$ gates. The $U_\xi^{2^\ell}$ gates are fed with their eigenstate $|u\rangle$ which remains unchanged all through the transformation. The control qubits terminate in the transformed states defined by the right-hand size of Eq. (A-1) where the normalization factors $1/\sqrt{2}$ have been omitted in the figure.

In the circuit of Fig. 6, the L input qubits, prepared in state $|+\rangle$, act as control qubits to the L controlled- $U_\xi^{2^\ell}$ gates, and terminate in the separable L -qubit state having the product form

$$|\hat{\psi}_\xi\rangle = \frac{1}{2^{L/2}} \left[|0\rangle + \exp(i2\pi 2^{L-1}\xi) |1\rangle \right] \left[|0\rangle + \exp(i2\pi 2^{L-2}\xi) |1\rangle \right] \cdots \left[|0\rangle + \exp(i2\pi 2^0\xi) |1\rangle \right] \quad (\text{A-2})$$

$$= \frac{1}{2^{L/2}} \bigotimes_{\ell=1}^L \left[|0\rangle + \exp\left(i2\pi j_\xi \frac{2^{L-\ell}}{2^L}\right) |1\rangle \right] \quad (\text{A-3})$$

$$= \frac{1}{2^{L/2}} \sum_{k=0}^{2^L-1} \exp\left(i2\pi \frac{j_\xi k}{2^L}\right) |k\rangle , \quad (\text{A-4})$$

with $j_\xi/2^L = \xi \Leftrightarrow j_\xi = \xi 2^L$. The state $|\hat{\psi}_\xi\rangle$ of Eq. (A-4) is similar in form to the state $|\tilde{\psi}_\xi\rangle$ of Eq. (6) with uniform coefficients $a_k = 1/\sqrt{N}$, and when $N = 2^L$.

The L -qubit state $|\hat{\psi}_\xi\rangle \in \mathcal{H}_2^{\otimes L}$ of Eq. (A-4) is then inverse Fourier transformed and then measured in the computational basis of $\mathcal{H}_2^{\otimes L}$. The measurement delivers an integer $j \in [0, 2^L - 1]$ and the phase estimate follows as $\hat{\xi} = j/2^L$.

This standard approach uses L qubits and it requires the L processes $U_\xi^{2^\ell}$ for every integer $\ell \in [0, L - 1]$, according to the circuitry of Fig. 6. This is equivalent to a total number of evaluations of the underlying elementary process U_ξ as $2^0 + 2^1 + 2^2 + 2^3 + \cdots + 2^\ell + \cdots + 2^{L-1} = 2^L - 1 = N - 1$. With such $\sim N$ evaluations of the elementary process U_ξ to be estimated, ensues a mean-squared estimation error scaling as $1/N$, known as the shot-noise or standard limit of the error.

As an alternative, our approach here uses a larger number $N - 1 = 2^L - 1$ of qubits, but a reduced circuitry requiring a single copy of the process U_ξ materialized by a single gate, according to Fig. 1. This single copy of U_ξ is evaluated a total of $N - 1$ times, sequentially for each of the $N - 1$ control qubits in Fig. 1. So our approach performs the same number $\sim N$ of evaluations of U_ξ and it achieves the same $1/N$ scaling of the mean-squared estimation error as the standard approach. Both approaches form two feasible alternatives associated with two distinct circuit implementations in Fig. 1 and in Fig. 6. In addition, by optimally selecting the coefficients a_k in Eq. (6), not present in the standard approach with Eq. (A-4), the possibility exists of achieving a reduced mean-squared estimation error scaling as $1/N^2$, known as the Heisenberg limit of the error, as shown in Section 3.

Appendix B: Optimal input superposition

For computing the estimation error with an arbitrary input superposition $|\psi_{\text{in}}\rangle$ in Eq. (5), we have, from Eq. (9), the measurement probability

$$P_j = |a'_j|^2 = {a'_j}^* a'_j \quad (\text{B-1})$$

$$= \frac{1}{N} \left[\sum_{k=0}^{N-1} a_k \exp\left(i2\pi \frac{(j_\xi - j)k}{N}\right) \right] \left[\sum_{\ell=0}^{N-1} a_\ell^* \exp\left(-i2\pi \frac{(j_\xi - j)\ell}{N}\right) \right] \quad (\text{B-2})$$

$$= \frac{1}{N} \sum_{k=0}^{N-1} \sum_{\ell=0}^{N-1} a_k a_\ell^* \exp\left(i2\pi \frac{(j_\xi - j)(k - \ell)}{N}\right) \quad (\text{B-3})$$

$$= \frac{1}{N} \sum_{k=0}^{N-1} \sum_{\ell=0}^{N-1} |a_k| |a_\ell| \cos\left[2\pi \left(\xi - \frac{j}{N}\right)(k - \ell) + \varphi_k - \varphi_\ell\right], \quad (\text{B-4})$$

since P_j is real, and with for each complex coefficient $a_k = |a_k| \exp(i\varphi_k)$.

To compute the estimation error $e_s^2(\hat{\xi})$ of Eq. (11) we have the average

$$\langle \cos[2\pi(\hat{\xi} - \xi)] \rangle = \sum_{j=0}^{N-1} P_j \cos\left[2\pi \left(\xi - \frac{j}{N}\right)\right] \quad (\text{B-5})$$

$$= \sum_{k=0}^{N-1} \sum_{\ell=0}^{N-1} |a_k| |a_\ell| W_{k\ell}, \quad (\text{B-6})$$

with

$$W_{k\ell} = \frac{1}{N} \sum_{j=0}^{N-1} \cos\left[2\pi \left(\xi - \frac{j}{N}\right)(k - \ell) + \varphi_k - \varphi_\ell\right] \cos\left[2\pi \left(\xi - \frac{j}{N}\right)\right]. \quad (\text{B-7})$$

The product of two cosines is then linearized as

$$W_{k\ell} = \frac{1}{2N} \sum_{j=0}^{N-1} \left\{ \cos\left[2\pi \left(\xi - \frac{j}{N}\right)(k - \ell + 1) + \varphi_k - \varphi_\ell\right] + \cos\left[2\pi \left(\xi - \frac{j}{N}\right)(k - \ell - 1) + \varphi_k - \varphi_\ell\right] \right\}. \quad (\text{B-8})$$

The two sums of cosines in Eq. (B-8) can be explicitly evaluated, via a geometric series of complex exponentials, and for the different integers $k, \ell \in [0, N - 1]$. We then arrive for the average of Eqs. (B-5)–(B-6) at

$$\langle \cos[2\pi(\hat{\xi} - \xi)] \rangle = \sum_{k=0}^{N-2} |a_{k+1}| |a_k| \cos(\varphi_{k+1} - \varphi_k) + |a_{N-1}| |a_0| \cos(2\pi N \xi + \varphi_{N-1} - \varphi_0). \quad (\text{B-9})$$

Based on Eq. (B-9), the estimation error of Eq. (11) can be made independent of the parameter ξ , which is an interesting property ensuring an intrinsic performance to the estimator $\hat{\xi} = j/N$ independent of the unknown phase ξ being estimated. This can be obtained in Eq. (B-9) by selecting for the input superposition the coefficient $a_0 = 0$. Then the average of Eq. (B-9) reduces to

$$\langle \cos[2\pi(\hat{\xi} - \xi)] \rangle = \sum_{k=0}^{N-2} |a_{k+1}| |a_k| \cos(\varphi_{k+1} - \varphi_k), \quad (\text{B-10})$$

affording in Eq. (11) the ξ -independent estimation error

$$e_s^2(\hat{\xi}) = \frac{1}{2\pi^2} \left[1 - \sum_{k=0}^{N-2} |a_{k+1}| |a_k| \cos(\varphi_{k+1} - \varphi_k) \right]. \quad (\text{B-11})$$

The next step for a good performance is to select the remaining coefficients a_k of the input superposition, so as to minimize the estimation error $e_s^2(\hat{\xi})$ in Eq. (B-11), or equivalently maximize the sum in Eq. (B-10), subject to the normalization constraint $\sum_{k=0}^{N-1} |a_k|^2 = 1$. The arguments φ_k in Eq. (B-10) are completely free angles not restricted by the normalization constraint. To maximize Eq. (B-10) they should therefore all be selected so that $\cos(\varphi_{k+1} - \varphi_k) = 1$ for all k ; and this can be obtained by $\varphi_k = 0$ for all k in Eq. (B-10). The maximum of Eq. (B-10) is thus achievable by a set of real coefficients $a_k \in \mathbb{R}$ in the input superposition; relative phase differences between them would be detrimental. For real coefficients a_k , the error of Eq. (B-11) can be written

$$e_s^2(\hat{\xi}) = \frac{1}{2\pi^2} \left(1 - \sum_{k=0}^{N-2} a_k a_{k+1} \right). \quad (\text{B-12})$$

The constrained minimization of Eq. (B-12) is accomplished by the coefficients

$$a_k = \sqrt{\frac{2}{N}} \sin\left(\pi \frac{k}{N}\right), \quad k = 0, 1, \dots, N-1, \quad (\text{B-13})$$

that satisfy the canonical equations of the Lagrange multiplier method. The same optimal coefficients as in Eq. (B-13) are also found in [25] or in [21] in somewhat distinct conditions of Fourier-based phase estimation as explained at the end of Section 3. From Eq. (B-13), the coefficients a'_j in Eq. (9) then take the form

$$a'_j = \frac{\sqrt{2}}{N} \sum_{k=0}^{N-1} \sin\left(\pi \frac{k}{N}\right) \exp\left[i2\pi \frac{(j_\xi - j)k}{N}\right]. \quad (\text{B-14})$$

This leads for the phase estimate $\hat{\xi}$ to the probability $\Pr(\hat{\xi} = j/N) = P_j = |a'_j|^2$ which, via explicit evaluation of the sum from Eq. (B-14), is

$$\Pr(\hat{\xi} = j/N) = \frac{1}{2N^2} \left[S_+^2 + S_-^2 + 2 \cos\left(\frac{\pi}{N}\right) S_+ S_- \right], \quad (\text{B-15})$$

with the two auxiliary sums

$$S_\pm = \frac{\sin\left(\frac{\pi}{2} [1 \pm 2(j_\xi - j)]\right)}{\sin\left(\frac{\pi}{2N} [1 \pm 2(j_\xi - j)]\right)}. \quad (\text{B-16})$$

The probability $\Pr(\hat{\xi} = j/N)$ of Eq. (B-15) is represented in Fig. 7.

It is verified in Fig. 7 that the distribution of probabilities $\Pr(\hat{\xi} = j/N)$ of Eq. (B-15) associated with the optimal nonuniform input superposition from Eq. (B-13) is, in generic conditions, more peaked around the true phase ξ than the distribution from Eq. (12) using a uniform input superposition instead, and consistently leads to a smaller estimation error.

In addition, the optimal nonuniform coefficients of Eq. (B-13) achieve in Eq. (B-10) the maximum $\cos(\pi/N)$, and this corresponds in Eq. (B-12) to the minimal estimation

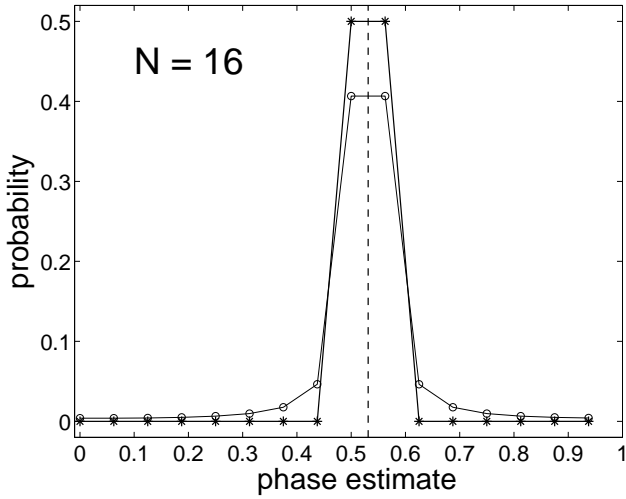


Fig. 7. The probability $\Pr(\hat{\xi} = j/N) = P_j = |a'_j|^2$ for the estimate $\hat{\xi}$ of the phase in abscissa, as it results : (*) from of Eq. (B-15) with the optimal input superposition of Eq. (B-13), or (o) from Eq. (12) with the non-optimal uniform superposition $a_k = 1/\sqrt{N}$. The size $N = 16$. The true value of the phase to be estimated is $\xi = 0.5 + 0.5/N$ shown by the vertical dotted line.

error

$$e_s^2(\hat{\xi}) = \frac{1}{2\pi^2} \left[1 - \cos\left(\frac{\pi}{N}\right) \right] = \frac{1}{\pi^2} \sin^2\left(\frac{\pi}{2N}\right) \quad (\text{B-17})$$

further used in Eq. (15).

References

- [1] M. A. Nielsen and I. L. Chuang, *Quantum Computation and Quantum Information*. Cambridge: Cambridge University Press, 2000.
- [2] J. Zhang, K. Li, S. Cong, and H. Wang, “Efficient reconstruction of density matrices for high dimensional quantum state tomography,” *Signal Processing*, vol. 139, pp. 136–142, 2017.
- [3] Y. Deville and A. Deville, “Blind quantum source separation: Quantum-processing qubit uncoupling systems based on disentanglement,” *Digital Signal Processing*, vol. 67, pp. 30–51, 2017.
- [4] F. Chapeau-Blondeau, “Optimization of quantum states for signaling across an arbitrary qubit noise channel with minimum-error detection,” *IEEE Transactions on Information Theory*, vol. 61, pp. 4500–4510, 2015.
- [5] Y. Deville, “ICA-based and second-order separability of nonlinear models involving reference signals: General properties and application to quantum bits,” *Signal Processing*, vol. 92, pp. 1785–1795, 2012.
- [6] Y. C. Eldar and A. V. Oppenheim, “Quantum signal processing,” *IEEE Signal Processing Magazine*, vol. 19, pp. 12–32, Nov. 2002.
- [7] Y. C. Eldar and G. D. Forney, “On quantum detection and the square-root measurement,” *IEEE Transactions on Information Theory*, vol. 47, pp. 858–872, 2001.

- [8] J. Zhang, S. Cong, Q. Ling, and K. Li, “An efficient and fast quantum state estimator with sparse disturbance,” *IEEE Transactions on Cybernetics*, vol. 49, pp. 2546–2555, 2019.
- [9] V. Giovannetti, S. Lloyd, and L. Maccone, “Advances in quantum metrology,” *Nature Photonics*, vol. 5, pp. 222–229, 2011.
- [10] C. L. Degen, F. Reinhard, and P. Cappellaro, “Quantum sensing,” *Reviews of Modern Physics*, vol. 89, pp. 035002,1–39, 2017.
- [11] P. W. Shor, “Polynomial-time algorithms for prime factorization and discrete logarithms on a quantum computer,” *SIAM Journal on Computing*, vol. 26, pp. 1484–1509, 1997.
- [12] P. Botsinis, D. Alanis, Z. Babar, H. Nguyen, D. Chandra, S. X. Ng, and L. Hanzo, “Quantum search algorithms for wireless communications,” *IEEE Communications Surveys & Tutorials*, vol. 21, pp. 1209–1242, 2019.
- [13] C. W. Helstrom, *Quantum Detection and Estimation Theory*. New York: Academic Press, 1976.
- [14] G. M. D’Ariano, C. Macchiavello, and M. F. Sacchi, “On the general problem of quantum phase estimation,” *Physics Letters A*, vol. 248, pp. 103–108, 1998.
- [15] M. G. A. Paris and J. Řeháček (Eds.), *Quantum State Estimation; Lecture Notes in Physics*, vol. 649. Berlin: Springer, 2004.
- [16] M. G. A. Paris, “Quantum estimation for quantum technology,” *International Journal of Quantum Information*, vol. 7, pp. 125–137, 2009.
- [17] R. Blume-Kohout, “Optimal, reliable estimation of quantum states,” *New Journal of Physics*, vol. 12, pp. 043034,1–25, 2010.
- [18] F. Chapeau-Blondeau, “Optimizing qubit phase estimation,” *Physical Review A*, vol. 94, pp. 022334,1–14, 2016.
- [19] A. Kitaev, “Quantum measurements and the Abelian stabilizer problem,” *arXiv.org e-print*, 1995. arXiv:quant-ph/9511026 (22 pages).
- [20] R. Cleve, A. Ekert, C. Macchiavello, and M. Mosca, “Quantum algorithms revisited,” *Proceedings of the Royal Society of London A*, vol. 454, pp. 339–354, 1998.
- [21] Z. Ji, G. Wang, R. Duan, Y. Feng, and M. Ying, “Parameter estimation of quantum channels,” *IEEE Transactions on Information Theory*, vol. 54, pp. 5172–5185, 2008.
- [22] D. W. Berry, B. L. Higgins, S. D. Bartlett, M. W. Mitchell, G. J. Pryde, and H. M. Wiseman, “How to perform the most accurate possible phase measurements,” *Physical Review A*, vol. 80, pp. 052114,1–22, 2009.
- [23] T. Kaftal and R. Demkowicz-Dobrzański, “Usefulness of an enhanced Kitaev phase-estimation algorithm in quantum metrology and computation,” *Physical Review A*, vol. 90, pp. 062313,1–6, 2014.
- [24] F. Chapeau-Blondeau, “Entanglement-assisted quantum parameter estimation from a noisy qubit pair: A Fisher information analysis,” *Physics Letters A*, vol. 381, pp. 1369–1378, 2017.
- [25] W. van Dam, G. M. D’Ariano, A. Ekert, C. Macchiavello, and M. Mosca, “Optimal quantum circuits for general phase estimation,” *Physical Review Letters*, vol. 98, pp. 090501,1–4, 2007.

- [26] J. M. Chappell, M. A. Lohe, L. von Smekal, A. Iqbal, and D. Abbott, “A precise error bound for quantum phase estimation,” *PLOS ONE*, vol. 6, pp. e19663,1–4, 2011.
- [27] T. E. O’Brien, B. Tarasinski, and B. M. Terhal, “Quantum phase estimation of multiple eigenvalues for small-scale (noisy) experiments,” *New Journal of Physics*, vol. 21, pp. 023022,1–28, 2019.
- [28] A. S. Holevo, *Probabilistic and Statistical Aspects of Quantum Theory*. Amsterdam: North-Holland, 1982.
- [29] B. T. Torosov and N. V. Vitanov, “Design of quantum Fourier transforms and quantum algorithms by using circulant Hamiltonians,” *Physical Review A*, vol. 80, pp. 022329,1–5, 2009.
- [30] R. Barak and Y. Ben-Aryeh, “Quantum fast Fourier transform and quantum computation by linear optics,” *Journal of the Optical Society of America B*, vol. 24, pp. 231–240, 2007.
- [31] L. E. Heyfron and E. T. Campbell, “An efficient quantum compiler that reduces T count,” *arXiv.org e-print*, 2018. arXiv:1712.01557 [quant-ph] (19 pages).
- [32] T. Häner, D. S. Steiger, K. Svore, and M. Troyer, “A software methodology for compiling quantum programs,” *Quantum Science and Technology*, vol. 3, pp. 020501,1–18, 2018.
- [33] B. L. Higgins, D. W. Berry, S. D. Bartlett, M. W. Mitchell, H. M. Wiseman, and G. J. Pryde, “Demonstrating Heisenberg-limited unambiguous phase estimation without adaptive measurements,” *New Journal of Physics*, vol. 11, pp. 073023,1–14, 2009.
- [34] B. M. Escher, R. L. de Matos Filho, and L. Davidovich, “General framework for estimating the ultimate precision limit in noisy quantum-enhanced metrology,” *Nature Physics*, vol. 7, pp. 406–411, 2011.
- [35] U. Dorner, R. Demkowicz-Dobrzanski, B. J. Smith, J. S. Lundeen, W. Wasilewski, K. Banaszek, and I. A. Walmsley, “Optimal quantum phase estimation,” *Physical Review Letters*, vol. 102, pp. 040403,1–4, 2009.
- [36] K. M. Svore, M. B. Hastings, and M. Freedman, “Faster phase estimation,” *Quantum Information and Computation*, vol. 14, pp. 306–328, 2013.
- [37] S. Kimmel, G. H. Low, and T. J. Yoder, “Robust calibration of a universal single-qubit gate-set via robust phase estimation,” *Physical Review A*, vol. 92, pp. 062315,1–13, 2015.
- [38] N. Wiebe and C. Granade, “Efficient Bayesian phase estimation,” *Physical Review Letters*, vol. 117, pp. 010503,1–6, 2016.
- [39] S. F. Huelga, C. Macchiavello, T. Pellizzari, A. K. Ekert, M. B. Plenio, and J. I. Cirac, “Improvement of frequency standards with quantum entanglement,” *Physical Review Letters*, vol. 79, pp. 3865–3868, 1997.
- [40] P. Kok, J. Dunningham, and J. F. Ralph, “Role of entanglement in calibrating optical quantum gyroscopes,” *Physical Review A*, vol. 97, pp. 012326,1–10, 2017.
- [41] F. Chapeau-Blondeau, “Optimized entanglement for quantum parameter estimation from noisy qubits,” *International Journal of Quantum Information*, vol. 16, pp. 1850056,1–25, 2018.